JOURNAL OF MATERIALS SCIENCE 39 (2004) 6921–6927

Titanium-doped γ-Fe_2O_3: Reduction and oxidation properties

I. AYUB, F. J. BERRY*, E. CRABB
Department of Chemistry, The Open University, Walton Hall, Milton Keynes MK7 6AA, U.K.
E-mail: f.j.berry@open.ac.uk

Ö. HELGASON
Science Institute, University of Iceland, Dunhagi 3, IS-107 Reykjavik, Iceland

Dedicated to Professor Philipp Gütlich on his seventieth birthday

Titanium-doped γ-Fe_2O_3 has been prepared by the calcination of a solid formed by the addition of aqueous ammonia to an aqueous solution of titanium- and iron-containing salts and boiling the precipitate under reflux. As compared to pure γ-Fe_2O_3 made by similar methods, titanium-doped γ-Fe_2O_3 showed a higher surface area and a greater stability to reduction, thermal conversion to an α-Fe_2O_3-related structure and the maintenance of a higher surface area during oxidation-reduction cycling.

1. Introduction

γ-Fe_2O_3 adopts a cubic close packed cation deficient spinel-related structure. The preparation of γ-Fe_2O_3 with controlled particle size is of special interest in various scientific and technological areas including those concerning magnetic solids and pigments and this has resulted in recent attempts to prepare nanoparticle materials by hydrolysis and pyrosol methods [1], inert gas condensation [2], and microwave plasma techniques [3]. More recently iron oxides have been shown to have reduction-reoxidation properties suitable for their use as oxygen storage components in automobile exhaust catalysts [4].

We have recently reported on the structural properties of iron oxides, particularly Fe_3O_4 and α-Fe_2O_3, when doped with tetravalent cations [5, 6]. We have now turned our attention to γ-Fe_2O_3-related systems and we report here on the synthesis of small particle γ-Fe_2O_3 doped with titanium and the effect of titanium on the surface area and stability of the material when treated under oxidising and reducing conditions.

2. Experimental

Iron (II) chloride tetrahydrate and iron (III) chloride hexahydrate in a molar ratio of iron (II) to iron (III) of 1:2 were dissolved separately in distilled water. The iron (II)-containing solution was added to the iron (III)-containing solution. An aqueous suspension of titanium tetrachloride was added to the iron-containing solution. Aqueous ammonia (40 cm^3) was added and the resultant precipitate boiled under reflux for 3 h. The precipitate was filtered, washed with 95% ethanol, dried under an infrared lamp and calcined in air at 250°C for 12 h. Pure γ-Fe_2O_3 was prepared by an identical method but without the addition of titanium tetrachloride.

X-ray powder diffraction patterns were recorded with a Siemens D5000 diffractometer in reflection mode using Cu K_α radiation. ^{57}Fe Mössbauer spectra were recorded with a microprocessor controlled Mössbauer spectrometer using a ca. 25 mCi ^{57}Co/Rh source. The instrument was calibrated using a natural iron standard. Chemical isomer shift data are referred to metallic iron. *In situ* ^{57}Fe Mössbauer spectra were recorded at elevated temperatures using a furnace described elsewhere [7]. Temperature programmed reduction profiles were recorded under a 10% hydrogen-90% nitrogen gas flow (20 $cm^3 min^{-1}$) with the temperature increasing linearly with time (5°C min^{-1}) and the consumption of hydrogen monitored with a kathrometer detector. Surface area measurements were determined by nitrogen gas adsorption at 77 K by the BET method using high vacuum conditions in a conventional apparatus.

3. Results and discussion

Pure γ-Fe_2O_3 prepared by the method described here was formed with a surface area of 69 $m^2 g^{-1}$.

The X-ray powder diffraction pattern recorded from the titanium-doped γ-Fe_2O_3 which was shown by ICP analysis to contain 4.04 wt% titanium was characteristic of a single phase material. Recent EXAFS studies of similarly produced samples [8] have indicated that titanium adopts the octahedral site in the spinel-related structure. The ^{57}Fe Mössbauer spectrum recorded from the material (Fig. 1) showed the superposition of a broadened sextet pattern ($\delta = -0.36(2)$ mms^{-1}, $\Delta = 0.00(2)$ mms^{-1}, $H = 43(2)$ T) and a doublet

*Author to whom all correspondence should be addressed.

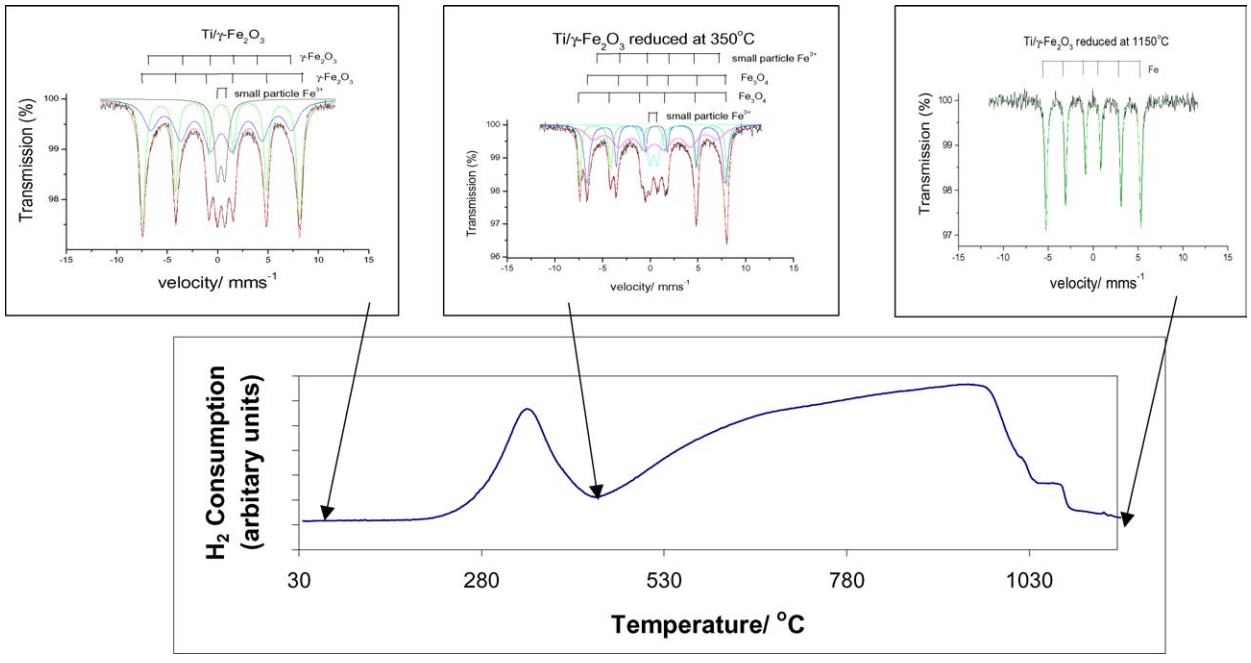

Figure 1 Temperature programmed reduction profile recorded from titanium-doped γ-Fe_2O_3 and the ^{57}Fe Mössbauer spectra recorded at 298 K following each reduction peak.

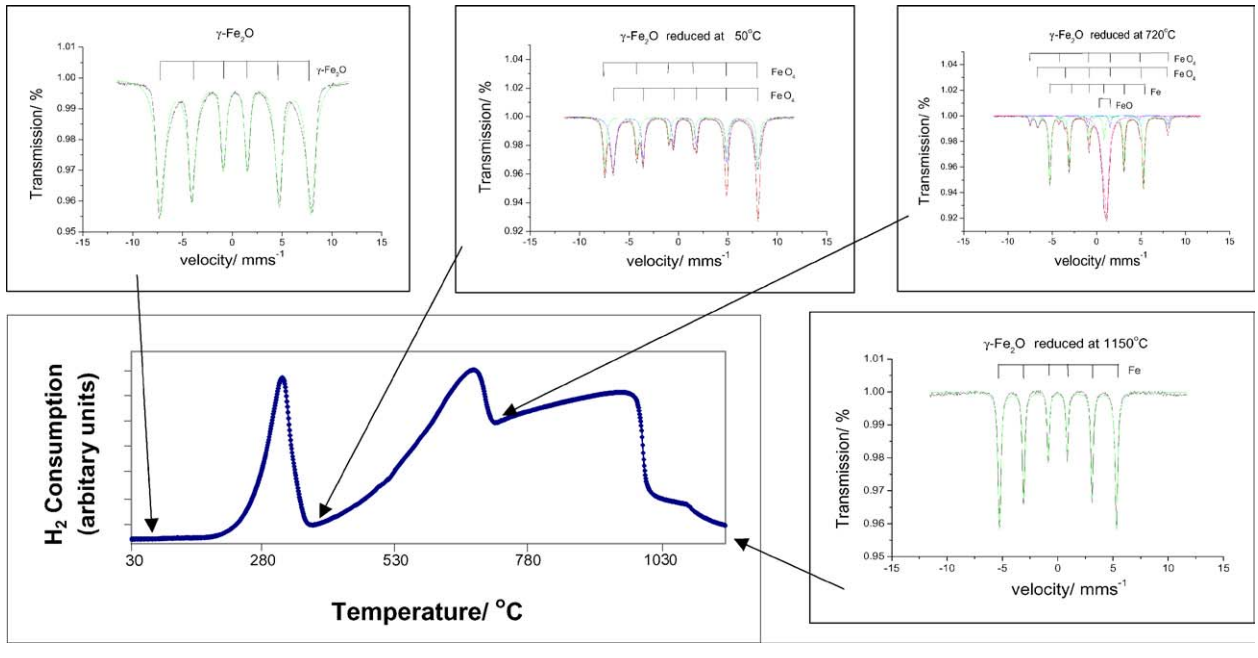

Figure 2 Temperature programmed reduction profile recorded from γ-Fe_2O_3 and the ^{57}Fe Mössbauer spectra recorded at 298 K following each reduction peak.

(δ = 0.35(2) mms^{-1}, Δ = 0.75(2) mms^{-1}) characteristic of small particle superparamagnetic iron oxide [9] on a sextet pattern (δ = 0.35(2) mms^{-1}, Δ = 0.01(2) mms^{-1}, H = 48(1) T). The presence of superparamagnetic particles was confirmed by the observation of only magnetic order in the sample when the spectrum was recorded at 80 K. The result is also consistent with our previous observation of superparamagnetic particles in γ-Fe_2O_3-related materials made by identical methods [8]. The observation in the ^{57}Fe Mossbauer spectrum of a significant amount (ca. 42%) of small particle iron oxide is consistent with the higher surface area (ca. 139 m^{2}g^{-1}) in the titanium-doped γ-Fe_2O_3. The larger particle size of the undoped material is also reflected by the virtual absence of the doublet corresponding to small particle superparamagnetic iron oxide in the ^{57}Fe Mossbauer spectrum from pure γ-Fe_2O_3 (Fig. 2).

3.1. Reduction properties

The temperature programmed reduction profile recorded from titanium-doped γ-Fe_2O_3 showed two reduction peaks (Fig. 1). The ^{57}Fe Mössbauer spectrum recorded *ex situ* after the first reduction peak at ca. 350°C (Fig. 1) showed the emergence of a new sextet (δ = ca. 0.7(1) mms^{-1}) accounting for ca. 30% of the total spectral area with a magnetic hyperfine field of

ca. 45(1) T. Another sextet pattern, H = ca. 48(1) T, corresponding to ca. 25% of the spectrum and a doublet amounting to ca. 10% of the total area could also be fitted. The remaining 35% of the spectral area was fitting using previously described methods [10] to a broad distribution of magnetic hyperfine fields covering the range ca. 38 to 43T with an average isomer shift of ca. 0.48 mms^{-1}. These was no facile way by which the distribution could be unequivocally related to either the sextet with large magnetic hyperfine field and isomer shift of ca. 0.3 mms^{-1} or the sextet with isomer shift of ca. 0.7 mms^{-1}. The sextet with the larger magnetic hyperfine field (H = ca. 48 T) has an isomer shift δ-ca. 0.35 mms^{-1} and quadrupole shift of nearly zero and is typical of Fe^{3+} ions in the tetrahedral A sites of Fe_3O_4. The sextet with a magnetic hyperfine field of ca. 45 T has an isomer shift δ = 0.7(0.1) mms^{-1} and is characteristic of an average charge of +2.5 for the iron ions in the octahedral B sites of Fe_3O_4 [11]. The third contribution with a wide range of magnetic hyperfine fields (ca. 40 T) observed in the spectrum recorded after the first reduction peak at ca. 350°C can be best associated with the effect of the particle size distribution [12]. The spectrum clearly shows a transition from the pure Fe^{3+}-containing γ-Fe_2O_3-related phase to the reduced variant in the form of a Fe_3O_4-related structure. An identical situation applies in the spectrum recorded from the undoped sample following initial reduction (Fig. 2). The distribution of particle sizes precludes interpretation in terms of the exact composition. The subsequent reduction of Fe_3O_4 proceeded over a large temperature range (Fig. 1) being completed at ca. 1100°C where the ^{57}Fe Mössbauer spectrum showed the formation of metallic iron (H = ca. 33 T) without the formation of iron-titanium oxides such as $FeTiO_3$. No evidence for titanium dioxide or a reduced form of titanium dioxide was observed in the X-ray powder diffraction pattern recorded following treatment in hydrogen at 1150°C. A comparison of the ^{57}Fe Mössbauer spectra and the temperature programmed reduction profile recorded from titanium-doped γ-Fe_2O_3 with those recorded from pure γ-Fe_2O_3 (Fig. 2) shows that in the undoped material initial reduction to Fe_3O_4(H = ca. 45 and 48 T) is also complete at ca. 350°C. However, following further treatment at ca. 720°C pure Fe_3O_4 underwent partial reduction to FeO (δ = 1.05(2) mms^{-1}, Δ = 0.29(2) mms^{-1}, ca. 40%) and metallic iron (H = 33(1) T, ca. 44%). The presence of Fe^{3+} and vacancies in nonstoichiometric FeO result in complex ^{57}Fe Mössbauer spectra [13] and unequivocal characterisation by Mössbauer spectroscopy is difficult especially in a multiphasic sample. However the X-ray powder diffraction pattern recorded *ex situ* after the second reduction peak at ca. 720°C showed three peaks at ca. 37°, 42° and 61° 2θ characteristic of FeO [14] together with reflections characteristic of Fe_3O_4 and metallic iron. The results also showed that reduction to metallic iron was complete at 1150°C. Hence

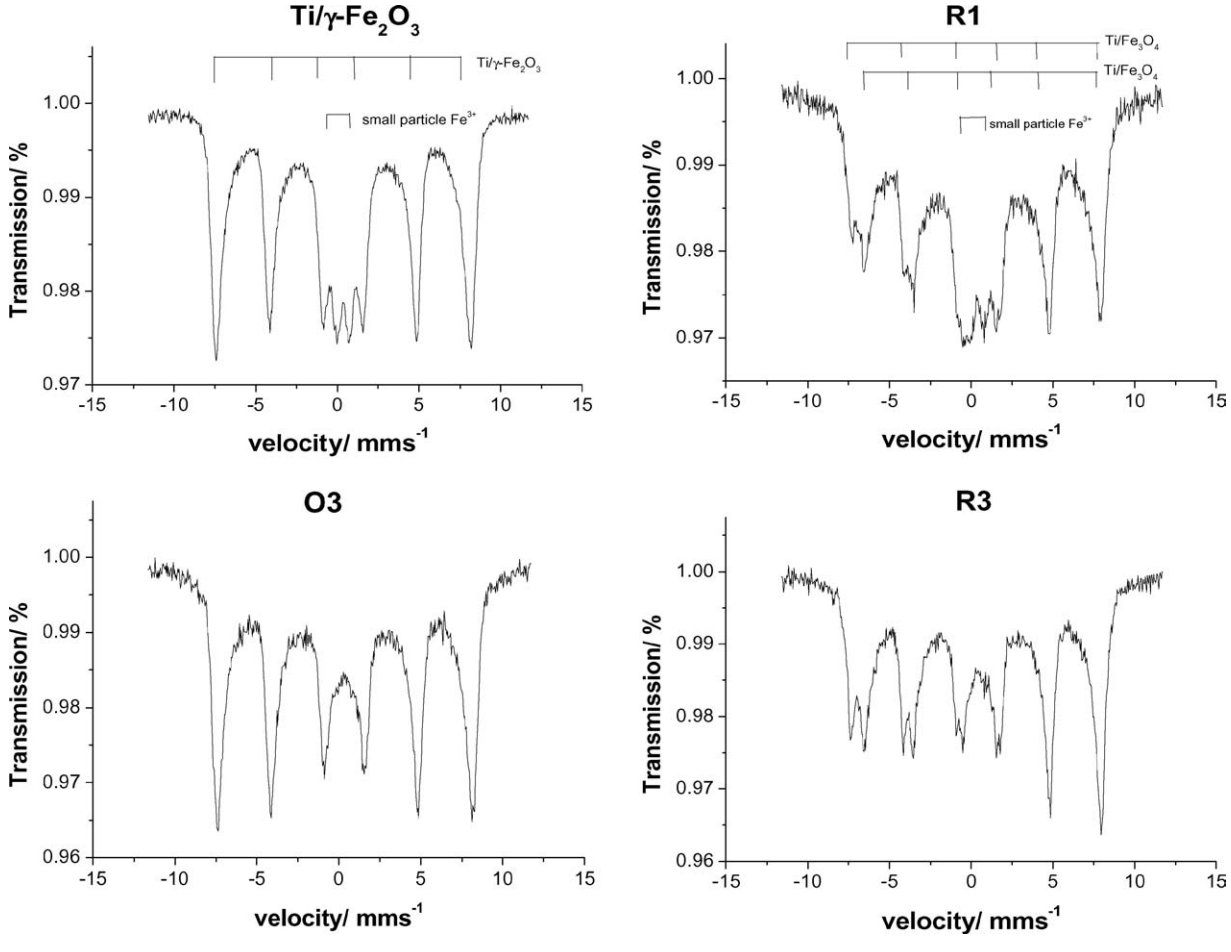

Figure 3 Some ^{57}Fe Mössbauer spectra recorded at 298 K from titanium-doped γ-Fe_2O_3 following reduction at 350°C in flowing 10% hydrogen-90% nitrogen (Rl); reoxidation by heating in air at 400°C (1 h) (01), and successive reduction, (R2, R3) and reoxidation (02, 03) treatment.

the presence of titanium in Fe_3O_4 appears to induce the steady consumption of hydrogen over a large temperature range and without the detectable formation of FeO.

3.2. Reduction—reoxidation properties

Titanium-doped γ-Fe_2O_3 was subjected to reduction at 350°C in the 10% hydrogen −90% nitrogen mixture (R1) and reoxidation by heating at 400°C for 1 h in air (01). The cycle of reduction and reoxidation was repeated twice (R2, 02, R3 and 03). Some ^{57}Fe Mössbauer spectra recorded *ex situ* from the reduced and reoxidised materials are collected in Fig. 3.

The titanium-doped γ-Fe_2O_3 was initially reduced (R1) to titanium-doped Fe_3O_4 ($H = 44(1)$ and 48(1) T) and reoxidised (01) to titanium-doped γ-Fe_2O_3 ($H = 47(1)$ T). The subsequent two fold reduction-reoxidation cycling (R2, 02, R3, 03) induced the formation of similar oxidised and reduced products. The main trend in the Mössbauer spectra was the simultaneous decrease in the intensity of the doublet and narrowing of the linewidths of the sextet patterns which indicated decreasing superparamagnetism resulting from an increase in particle size. The particle size of titanium-doped Fe_3O_4 (R1) of ca. 19 nm formed by initial reduction of titanium-doped γ-Fe_2O_3 was larger than that of the precursor titanium-doped γ-Fe_2O_3 (ca. 12 nm). The surface area of titanium-doped Fe_3O_4 (R1) of ca. 99 m^2g^{-1} was lower than that of titanium-doped γ-Fe_2O_3 (ca. 139 m^2g^{-1}). The results recorded from titanium-doped Fe_3O_4 (R1) compare well with those reported earlier for a material of composition $Fe_{2.5}Ti_{0.5}O_4$ [12]. Reoxidation by heating at 400°C for 1 h. in air followed by reduction and reoxidation for a further two cycles produced only small variations in particle size and surface area with the finally regenerated titanium-doped γ-Fe_2O_3 (03) having a particle size of ca. 18 nm and surface area of ca. 67 m^2g^{-1}. Identical reduction-reoxidation cycling was also performed on pure γ-Fe_2O_3 formed by similar methods. The surface area decreased from ca. 69 m^2g^{-1} for γ-Fe_2O_3 to ca. 29 m^2g^{-1} for Fe_3O_4 formed by initial reduction (R1). This was followed by reoxidation to γ-Fe_2O_3 (01) with slightly larger particle size (ca. 48 nm) and lower surface area (ca. 15 m^2g^{-1}). Repeating the reduction-reoxidation process over two cycles gave further small increases in particle size with the finally regenerated γ-Fe_2O_3 having a particle size of ca. 55 nm and surface area of ca. 15 m^2g^{-1}. Hence the results show that the incorporation of titanium within γ-Fe_2O_3 has a significant effect in inhibiting both particle growth and loss of surface area during reduction-reoxidation cycling within the temperature range examined.

3.3. Oxidation monitored *in situ* by ^{57}Fe Mössbauer spectroscopy

The ^{57}Fe Mössbauer spectra recorded *in situ* from titanium-doped Fe_3O_4 formed by reduction of titanium-doped γ-Fe_2O_3 and heated in an oxygen partial pressure of ca. 1 Pa are shown in Fig. 4. The ^{57}Fe Mössbauer

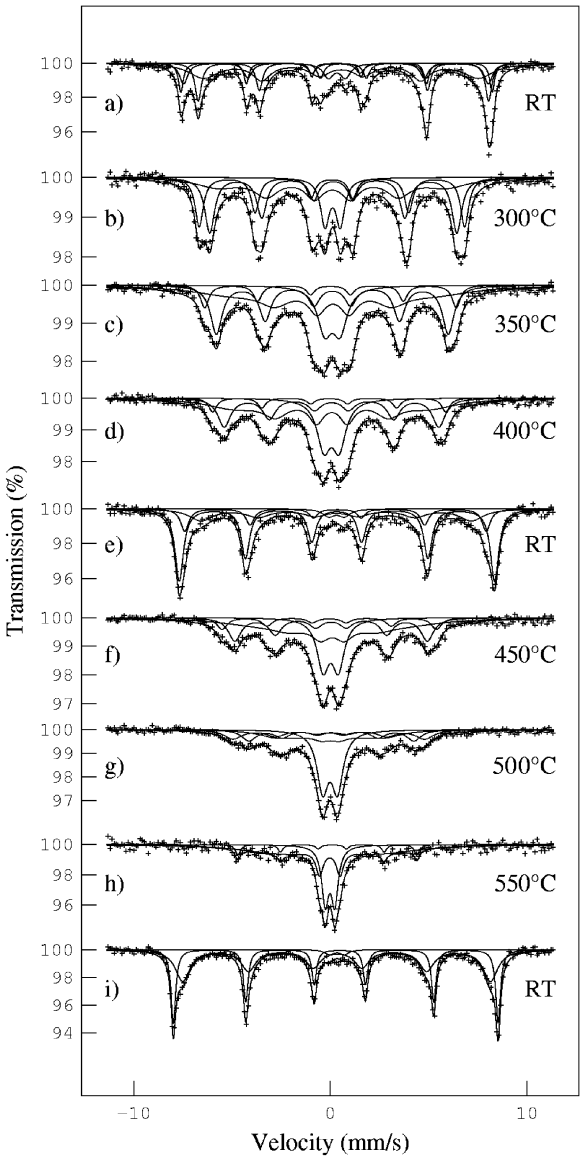

Figure 4 ^{57}Fe Mössbauer spectra recorded *in situ* from titanium-doped Fe_3O_4 following heating in an oxygen partial pressure of ca. 1 Pa.

parameters of the principal spectra are collected in Table I. The spectrum recorded at room temperature and shown in Fig. 4a is slightly different from the second spectrum in Fig. 1 and demonstrates that only partial reduction was achieved. The spectrum was best fitted to four sextets and one doublet accounting for ca. 6% of the spectral area. One of the sextets can be attributed to the A-site in titanium-doped Fe_3O_4 (as described above and in [11]) and another to a sextet which is characteristic of γ-Fe_2O_3. These sextets account for ca. 30% of the spectral area and are grouped together in Table I since Mössbauer spectroscopy is unable to distinguish between non-stoichiometric Fe_3O_4 and a mixture of Fe_3O_4 and γ-Fe_2O_3 [15] and the unambiguous deconvolution of the sextet with H = ca. 49 T into two discrete sextets corresponding to Fe^{3+} in γ-Fe_2O_3 and Fe^{3+} in Fe_3O_4 is therefore inappropriate. The third sextet accounting for ca. 22% of the spectral area is assigned to the B-site in Fe_3O_4 and has the expected hyperfine parameters (δ = ca.0.67 mms^{-1}, 2ε = ca.0.00 mms^{-1}, H = ca. 45 T). Finally, the broad-lined sextet δ = ca. 0.55 mms^{-1},

TABLE I ^{57}Fe Mössbauer parameters obtained from the fitting of the Mössbauer spectra in Fig. 4

	γ-Fe_2O_3-related sextet[a] or Fe_3O_4-related A-sextet[b]				Fe_3O_4-related B-sextet[b]					Low field distribution as a broad-line sextet				Doublet			
Temp. (°C)	δ/mms^{-1} (±0.03)	Γ/mms^{-1} (±0.1)	HT(±1)	Area% (±3)	δ/mms^{-1} (±0.03)	Δ/mms^{-1} (±0.02)	gΓ/mms^{-1} (±0.01)	HT(±1)	Area% (±3)	δ/mms^{-1} (±0.03)	Γ/mms^{-1} (±0.1)	H/T (±3)	Area% (±3)	gδ/mms^{-1} (±0.03)	gΔ/mms^{-1} (±0.1)	Γmms^{-1} (±0.1)	Area% (±3)
25 (4a)	0.31	0.5	49	30	0.67		0.5	45	22	0.55	1.8	41	42	0.33	0.7	0.9	6
25 (4e)	0.33	0.5	49	71						0.31	1.4	43	25	0.32	0.7	0.8	4
450 (4f)	−0.0	0.9	33	35						0.1	3	23	42	0.02	0.7	0.8	23
500 (4g)	−0.02	1.1	29	39						0	2.2	17	25	−0.01	0.7	0.8	36
523 (4h)					−0.03	−0.24	0.3	28	9[b]	−0.04	3.9	21	59	−0.02	0.5	0.5	32
25 (4i)	0.34	0.9	49	56	0.38	−0.21	0.3	51.3	41[b]					0.33	0.6	0.8	3

[a]The quadrupole shift was 0.0 ± 0.1 mms^{-1} in all spectra.
[b]Parameters for the α-Fe_2O_3-related sextet which appears during heating at 523°C.

$H =$ ca. 43 T is characteristic of the presence of the wide range of particle sizes which produces a broad magnetic hyperfine field distribution. The effect of the doping could not be distinguished separately in the fitting procedure.

The spectra in Fig. 4 recorded *in situ* at 300, 350 and 400°C (Fig. 4b, c and d) were each recorded for 6–8 h. They showed increasing overlap of the sextets with high magnetic hyperfine fields and a simultaneous change in the average isomer shift reflecting the growth of an Fe^{3+}-containing phase as the temperature increased. The area of the doublet and of the broad-line sextet with smaller magnetic hyperfine field also increased and accounted for ca. 65% of the area in the spectrum recorded from the material heated at 400°C. The oxidation was confirmed by the spectrum recorded when the material was cooled to room temperature (Fig. 4e) where the average isomer shift for all components was ca. 0.33 mms^{-1} as compared to ca. 0.48 mms^{-1} in Fig. 4a and where about 70% of the spectral area in the oxidised phase could be assigned to a γ-Fe_2O_3- related phase (2ε = ca.0.00(2) mms^{-1}, H = ca. 49(1) T). The spectrum was not amenable to fitting with a sextet corresponding to the B-site.

Further heating at 450 and 500°C gave spectra (Fig. 4f and g) which showed a continuation of the trend observed in the spectra Fig. 4b–d being composed of a broadened sextet pattern together with a dominant doublet contribution. At 500°C the doublet accounted for ca. 36% of the total spectral area. The spectrum recorded during treatment at 523°C (Fig. 4h) showed a gradual collapse of the broadened sextet pattern associated with the γ-Fe_2O_3-related phase together with two further effects. Firstly, ca. 32% of the spectrum was composed of a doublet corresponding to a paramagnetic species with sharper linewidths ($\Gamma = 0.5\ mms^{-1}$) and a well defined isomer shift ($\delta = -0.02\ (2)\ mms^{-1}$) and quadrupole splitting ($\Delta = 0.49(0.03)\ mms^{-1}$). Secondly, a sextet component characteristic of an α-Fe_2O_3-related phase with a magnetic hyperfine field H = ca. 28(2) T, and quadrupole shift of $-0.24(0.02)$ mms^{-1} and accounting for ca. 9% of the spectral area appeared. Attempts to refit the spectrum recorded at 500°C with the parameters characteristic of α-Fe_2O_3 were unsuccessful indicating that the phase transition to α-Fe_2O_3 begins at temperatures exceeding 500°C. Finally, the spectrum recorded after cooling to room temperature (Fig. 4i) confirmed the γ- to α-Fe_2O_3 phase transition with the sextet characteristic of α-Fe_2O_3 (H = ca. 51(1) T, $\Delta = -0.21(0.02)$ mms^{-1}) accounting for ca. 41% of the spectrum. The X-ray powder diffraction pattern recorded from the sample cooled to room temperature confirmed that titanium, either in the form of titanium dioxide or (less likely) $FeTiO_3$, had not segregated from the iron oxide during the thermal treatment.

The results contrast with those recorded from Fe_3O_4 formed by reduction of γ-Fe_2O_3 when heated in an oxygen partial pressure of ca. 1 Pa and which were similar to those reported previously [16]. The Fe_3O_4 was initially converted to γ-Fe_2O_3 at 200°C which appeared as a broad-lined spectrum. Cooling the sample to room temperature confirmed the identity of the material as γ-Fe_2O_3 ($H = 49(1)\ T$). Heating to 300°C showed the onset of α-Fe_2O_3 formation, which is in good agreement results obtained elsewhere [1, 12]. The spectrum recorded after cooling to room temperature showed the superposition of sextets corresponding to γ-Fe_2O_3 ($H = 49(1)\ T$) and α-Fe_2O_3 ($H = 52(1)\ T$). Further heating increased the intensity of the peaks corresponding to α-Fe_2O_3 until, at 427°C, the material was completely converted to α-Fe_2O_3 ($H = 52(1)\ T$).

The apparent stabilization by titanium of the conversion of spinel-related γ-Fe_2O_3 to its corundum-related α-Fe_2O_3 polymorph was confirmed by recording X-ray powder diffraction patterns *ex situ* from the samples following cooling to room temperature. The results showed that the onset of conversion of titanium-doped γ-Fe_2O_3 of surface area 139 m^2g^{-1} to titanium-doped α-Fe_2O_3 occured at ca. 650°C and that conversion is complete at ca. 700°C. In contrast γ-Fe_2O_3 with a similar surface area (150 m^2g^{-1}) was converted to α-Fe_2O_3 at temperatures between 400 and 450°C. The results showed that the stabilization of the spinel-related γ-Fe_2O_3 structure with respect to its thermally induced conversion to α-Fe_2O_3, is a result of the presence of titanium as opposed to the higher surface area of the γ-Fe_2O_3-related phase.

4. Conclusion

Spinel-related titanium-doped γ-Fe_2O_3 prepared by the calcination of a solid formed by the addition of aqueous ammonia to an aqueous solution of titanium- and iron-containing salts and boiling the precipitate under reflux has a higher surface area but a greater stability to reduction and thermal conversion to a corundum-related α-Fe_2O_3- related material than its undoped counterpart. Titanium-doped γ-Fe_2O_3 also maintains a higher surface area during oxidation-reduction cycling.

Acknowledgement

We thank Johnson Matthey plc for financial support.

References

1. E. HERRERO, M. V. CABANAS, M. VALLET-REGI, J. L. MARTINEZ and J. M. GONZALEZ-CALBET, *Solid State Ionics* **101–103** (1997) 213.
2. G. SCHIMANKE and M. MARTIN, *ibid.* **136–137** (2000) 1235.
3. E. PELLEGRIN, M. HAGELSTEIN, S. DOYLE, H. O. MOSER, J. FUCHS, D. VOLLATH, S. SCHUPPLER, M. A. JAMES, S. S. SAXENA, L. NIESEN, O. ROGOJANN, G. A. SAWATZKY, C. FERRERO, M. BOROWSKY, O. TJERNBERG and N. B. BROOKES, *Phys. Stat Sol.* **215** (1999) 797.
4. J. M. FISHER, T. J. HYDE and D. THOMPSETT, UK Patent PCT/GB98/00325 (1998).
5. F. J. BERRY, C. GREAVES, J. G. MCMANUS, M. MORTIMER and G. OATES, *J. Solid State Chem.* **130** (1997) 272.
6. F. J. BERRY, C. GREAVES, Ö. HELGASON and J. G. MCMANUS, *J. Mater. Chem.* **9** (1999) 223.
7. Ö. HELGASON, H. P. GUNNLAUGSSON, K. JONSSON and S. STEINTHORSSON, *Hyperf. Inter.* **91** (1994) 595.
8. Ö. HELGASON, J.-M. GRENECHE, F. J. BERRY, S. MØRUP and F. MOSSELMANS, *J. Phys. Cond. Matter* **13** (2001) 10785.

9. F. J. BERRY, in "The Mössbauer Effect in Supported Microcrystallites," Advances in Inorganic Chemistry and Radiochemistry, Vol. 21, edited by H. J. Emeleus and A. G. Sharpe (Academic Press, New York, 1978), p. 255.
10. C. WIVEL and S. MØRUP, *J. Phys. E* **14** (1981) 605.
11. H. TANAKA and M. KONO, *J. Geomag. Geoelectr.* **39** (1987) 463.
12. N. GUIGUE-MILLOT, S. BÉGIN-COLIN, Y. CHAMPION, M. J. HŸTCH, G. LE CAËR and P. PERRIAT, *J. Solid State Chem.* **170** (2003) 30.
13. E. MURAD and J. M. JOHNSTON, in "Iron Oxides and Oxyhydroxides," Mössbauer Spectroscopy Applied to Inorganic Chemistry, Vol. 2, edited by G. J. Long (Plenum Press, New York, 1987) p. 507.
14. JCPDS Index No. 06-0615.
15. G. M. DA COSTA, E. DE GRAVE, P. M. A. DE BAKKER and R. E. VANDENBERGHE, *Clays Clay Mines.* **43** (1995) 656.
16. F. J. BERRY, Ö. HELGASON, K. JONSSON and S. J. SKINNER, in Proceedings of The International Conference on the Applications of the Mossbauer Effect, edited by I. Ortalli (SIF, Bologna, 1996) p. 59.
17. P. PERRIAT, E. FRIES, N. MILLOT and B. DOMENICHINI, *Solid State Ionics* **117** (1999) 175.

Received 17 November 2003
and accepted 12 July 2004